COVER SHEET

NOTE: This coversheet is intended for you to list your article title and author(s) name only —this page will not appear on the CD-ROM.

Paper Number: **384**

Title: **Numerical Simulation with Experimental Validation of the Draping Behavior of Woven Fabrics**

Authors: William R. Rodgers
Praveen Pasupuleti
Selina Zhao
Terry Wathen
Mark Doroudian
Venkat Aitharaju

<<All text below on this page can be deleted >>

(FIRST PAGE OF ARTICLE – *align this to the top of page – leave space blank above ABSTRACT*)

ABSTRACT

Woven fabric composites are extensively used in molding complex geometrical shapes due to their high conformability compared to other fabrics. Preforming is an important step in the overall process. In this step, the two-dimensional fabric is draped to become the three-dimensional shape of the part prior to resin injection. During preforming, the orientation of the tows may change significantly compared to the initial orientations. Accurate prediction of the tow orientations after molding is important for evaluating the structural performance of the final part.

This paper investigates the fiber angle changes for carbon fiber woven fabrics during draping over a truncated pyramid tool designed and fabricated at the General Motors Research Labs. This aspect of study is a subset of the broad study conducted under the purview of a Department of Energy project funded to GM in developing state of the art computational tools for integrated manufacturing and structural performance prediction of carbon fiber composites. Fabric bending, picture frame testing, and bias-extension evaluations were carried out to determine the material parameters for these fabrics. The PAM-FORM computer program was used to model the draping behavior of these fabrics. Following deformation, fiber angle changes at different locations on the truncated pyramid were measured experimentally. The predicted angles matched the experimental results well as measured along the centerline and at several different locations on the deformed fabric.

Details of the test methods used as well as the numerical results with various simulation parameters will be provided.

William R. Rodgers, Selina Zhao, Terry Wathen and Venkat Aitharaju; General Motors Global Research and Development Center, 30500 Mound Road, MC:106-224-RL1, Warren, MI 48092
Praveen Pasupuleti, Mark Doroudian; ESI North America, 32605 West 12 Mile Road #350, Farmington Hills MI 48334

INTRODUCTION

Woven fabrics as reinforcements for structural composites have gained significant interest in the composites community due to their improved stiffness and strength compared to non-crimp fabrics in the through-thickness direction. These fabrics are an excellent choice to mold components with complex geometry due to their high degree of drapeability. One of the challenges of using these fabrics in high volume manufacturing is the process quality assessment at various stages, such as fabric production, preform preparation, and molding. Preforming is one of the most important steps as it involves deforming a 2-D fabric into the complex 3-D shape of the final component. This operation can introduce changes in the fiber angles, fiber volume fraction, and thickness of the fabric, contributing to significant differences in local permeability and loss of mechanical properties in a given direction. Predicting these changes accurately during the preforming stage and accounting for them appropriately in the manufacturing and structural models is necessary to predict the outcome successfully.

In the literature, several methods were reported to detect the fiber orientation of 3-D draped fabrics during the preforming process. Researchers used optical methods to study the evolution of the tow directions for different loading cases such as tension, bias-tension, biaxial, picture frame and compression [1-3]. Analytical approaches for predicting the draping behavior can be classified broadly into kinematic, discrete and continuum damage mechanics based models. Kinematic models are pure geometrical mapping models and do not account for friction, loads, and boundary conditions [4-5]. In discrete models [6], the fiber tows are modeled with a mass and rotational rigidity and are connected by inextensible bars to form a two-dimensional truss. The potential energy of the system was derived based on the discrete kinematic variables of the truss and the equilibrium shape of the fabric draped over rigid surfaces was obtained by minimizing the potential energy. In the realm of continuum damage mechanics, several models were developed accounting for the fabric behavior in the meso and micro scales. Shell elements were used to model the woven fabric accounting for the bending and shear behavior in Yu, et al., Boisse, et al., and Xue, et al. [7-9]. Uni-axial, biaxial tension, picture frame, and bias-extension experiments were used to determine the material parameters for the simulation model. Researchers also studied the draping behavior of fabrics by modeling the tows explicitly using continuum 3D hexagonal elements [10-11]. In these papers, the fibrous behavior of the fabric was accounted for by appropriate constitutive laws. The contact behavior between the tows was simulated using gap elements. Recently, a new concept based on digital elements was developed by treating the tows as bundle of virtual fibers to account for the realignment of fibers during the loading [12-13]. Using these models, it is possible to model complex deformation of the tows, such as realignment of fibers during the low compaction pressure stage and transverse deformation of the tow only after full compaction. These digital models are still in the research stage and are not yet available for use in industrial applications.

In this paper, the draping behavior of different types of woven fabrics (satin and twill) with different orientations were studied both experimentally and numerically. The numerical approach follows the continuum damage models using shell elements developed in the commercial finite element program, PAM-FORM. Detailed fabric characterization tests such as cantilever bending and bias-extension, were conducted on the dry fabrics to derive material parameters for the simulation. A truncated pyramid tool was used to conduct the draping experiments. Numerical predictions for the fiber angle changes were compared with experimental measurements at several locations on on the truncated pyramid component and results are presented.

EXPERIMENTAL

Materials

Both carbon fiber fabrics used in this study were obtained from Sigmatex High Technology Fabrics, Inc. (Benicia, CA). These fabrics were woven from T700SC-12000 carbon fiber (Torayca fiber from Toray Industries, Inc., Japan). The fabrics were a 2x2 twill (TC-411, thickness - 0.48 mm, areal mass - 380 g/m^2) and a 5-Harness Satin (SC685, thickness – 0.52 mm, areal mass – 385 $g.m^2$). Squares of the fabric measuring 470 mm x 470 mm were excised from the roll of fabric using a Gerber Scientific model DCS2500 cutting table. While a large number of global orientations are possible for locating the fabric in the tool, for these experiments we limited the global orientations to two: 0/90° and +/- 45°.

Bias Extension Experiments

The bias extension test measures the load required to stretch fabric that is prepared with the fibers oriented at +/-45° with respect to the loading direction. This provides information on the way in which the load varies as the fibers reorient to different relative angles [14]. The bias extension test was carried out using specimens of each woven fabric. In order to simplify the analysis of the data, the length of the specimen was limited to 3 times the width. Therefore, the tested area of the fabric was 127 mm x 381 mm. Since the specimens required an extra 25 mm at each end in order to mount them in the grips of the test frame, the actual specimen length was 432 mm.

To ensure all of the fabric tows were engaged during testing, the last 25 mm of the fabric was tabbed between appropriately sized sections of 3 mm thick Garolite sheet that was attached using a liberal amount of Airtac 2 spray adhesive from Airtech International.

Great care was taken not to disturb the original fiber crossing angles of the test specimens as the specimens were prepared and mounted in the testing frame. Physical testing was performed on an Instron 5582 load frame using series 2710-116 side action grips with 25 mm x 76 mm grip faces. The grip separation rate during the testing was 30 mm/min.

Figure 1 presents images of one of the twill fabric specimens before and during the bias extension test. Figure 1(a) shows the specimen prior to the start of the test. From this image, it is clear that the fibers of the fabric run at +/- 45° to the direction of the test. Figure 1(b), shows the same specimen after 100 mm of extension. Clearly, no fiber pullout from the tabbed area was observed and the specimen has taken the classical shape observed during bias extension tests.

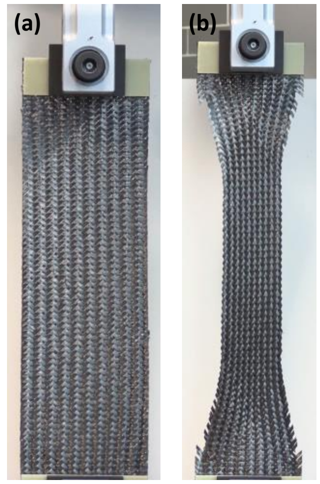

Figure 1. (a) 127 mm wide Twill Fabric at the start of the Bias Tension Test.
(b) The same Twill Fabric following 100 mm extension.

Deformation of Fabrics on the Preforming Tool

Since preforming is an important step in the overall process, a lab level truncated pyramid preforming tool was designed and fabricated at the GM Research Laboratories. Shown in Figure 2a and b, the preforming tool consists of a steel truncated pyramid male side, and a thick silicone rubber vacuum bag. A vacuum port is located at the center of the pyramid top surface. The orientation of the fabric (0/90 global or +/-45 global) was determined prior to cutting.

In order to lock in the shape of the fabric and the fiber directions following preforming, a Hexion thermoset powder binder was applied at a concentration of 1.5% by weight to the fabric. After the powder binder was uniformly applied to the fabric, the fabric was placed on the truncated pyramid tool in a freely draping position as shown in the Figure 2c. The vacuum bag was then carefully placed over the free fabric. The edges of the bag were sealed to the steel plug using vacuum grease. Following the placement of the silicone bag, a vacuum was pulled on the system. This deformed the fabric to the contour of the truncated pyramid. The entire system was then placed in a 120°C oven for 20 minutes under vacuum to consolidate the preform completely.

After this time, the preform tool was removed from the oven and allowed to cool under vacuum after which the vacuum was discontinued and the vacuum bag removed. The resulting single layer preform is shown in the Figure 2d. Then measurements were made on the orientation of the fibers while still attached to the preform tool.

Fiber Angle Measurements

Measuring the fiber crossing angles started with capturing a high resolution photographic image of the fabric that had been deformed over the preforming tool described above. Each image used for measurement included in it a 25.4 mm wide Post-it® tab that was used to calibrate the relationship between pixels and millimeters represented in the photographic image. With this calibration, it was possible to define an X-Y grid on the surface to be measured in order to determine the position of the

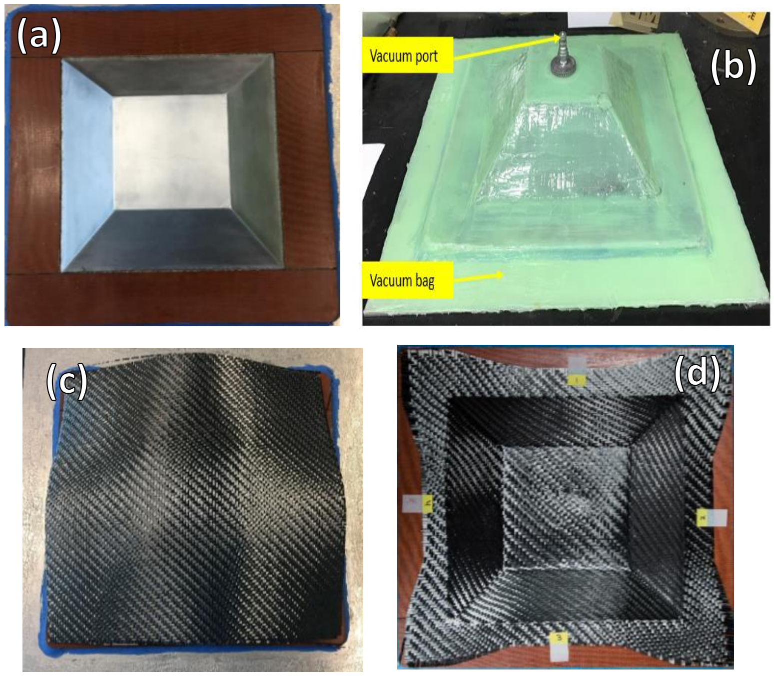

Figure 2. (a) The steel preforming tool. (b) Vacuum bagging applied onto the fabric. (c) Freely draping twill fabric in a global 0/90 orientation on top of the preform tool. (d) A single layer of global twill 0/90° fabric after preforming

measured fiber shear angles. This involved placing reference lines on the image at the bottom and top of the face of the truncated pyramid. Additional lines were added at the centerline of the face being measured, and at roughly the ¼, ½, and ¾ mark for distances up the face. It was possible to assign X-Y coordinates to the measurement location using this grid system.

Fiber angles were measured using an image analysis program, Image J, created by the National Institute of Health (http://imagej.nih.gov/ij/) [15]. This image analysis software has a tool that allows the angle of a manually drawn pair of intersecting lines to be measured. The fiber crossing angles were measured on the deformed fabric at locations along the grid as described above. Multiple measurements were conducted for each measurement location. While the position of these measurements does vary somewhat, they are usually taken from the same crossing point of two tows of fibers. The absolute value of the measured angles minus 90° were then charted using their X-position in order to visualize the changes in fiber angle across the face of the truncated pyramid.

RESULTS AND DISCUSSION

This paper discusses the comparison of experimentally measured fiber shear angle changes to simulations made using material model MAT-140 available in the PAM-FORM software. Previous work by the authors showed that a reasonable fit could be obtained through measurement of the bending stiffness of the fabrics and inverse modeling of the shear modulus for the woven fabrics [16]. This was done due to substantial inconsistency in the attempted measurement of the shear modulus parameters using a picture frame experimental evaluation. While reasonably good fits were obtained for twill fabrics in a 0/90° starting orientation, the match of the simulated parameter for the satin fabric needed to be improved. We therefore decided to approach the topic again using a different test to evaluate the shear modulus of the woven fabrics.

Calibration of PAM-FORM Material Model MAT-140

The PAM-FORM material model, MAT 140, was used to simulate the draping of dry woven carbon fabrics. The deformation modes in MAT 140 are defined on the level of the plies. The primary input parameters for the model are:

- Intra-ply shear - The shear stiffness of a fabric is an independent property. Shear stiffness is the most important factor because fabrics predominantly deform under this mode. A non-linear shear stiffness can be imposed via a test curve function. Currently, there are two test methods available for fabric shear testing. These are the picture frame and the bias extension tests. Either of these tests could be used to calibrate the shear modulus properties of a fabric for the MAT-140 model.
- Out-of-plane bending - Fabric bending stiffness is decoupled from in-plane stiffness and may be properly characterized via different methods. This parameter is often evaluated by the use of a Pierce Cantilever Bending apparatus. This parameter has been previously reported for the materials used in this work [16].
- Inter-ply sliding (friction)

The shape and deformation of a fabric is a combination of two or more modes, and depending on the type of fabric, one deformation mode may be dominant over the others.

Analysis of Bias Extension Experiments

The PAM-FORM MAT-140 model was used to characterize the bias-extension tests performed at General Motors. Both twill and satin fabrics were tested under controlled test conditions as discussed in the experimental section.

A half-symmetry model of the specimen was used to characterize the shear behavior for the different materials. The fiber directions in the model were oriented at +/-45° to

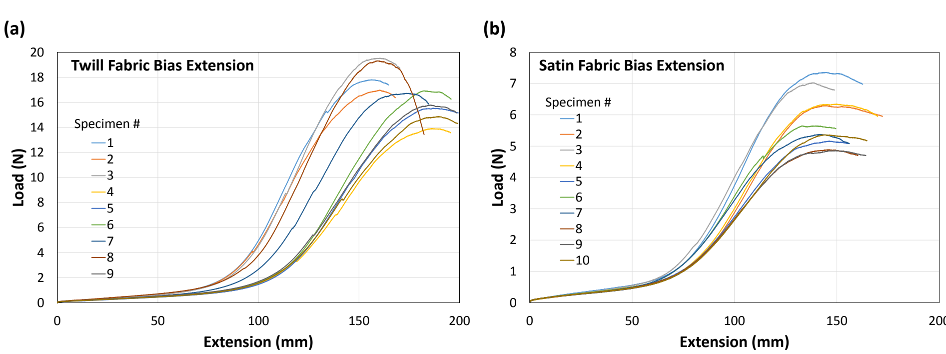

Figure 3. Force-deflection curves from bias-extension tests. (a) Twill fabric, (b) Satin fabric

the loading direction as per the test set-up. Figure 3 shows the load – extension curves for multiple specimens of the twill and satin fabrics.

A mean coupon response was selected from the set (Coupon-7 for twill and Coupon-6 for satin) and processed. The force-deflection data from the bias-extension test was converted to a shear stress-shear strain response and was provided as an input to the PAM-FORM material model to represent the shear behavior.

The force-deflection data used for the conversion was limited to 90 mm extension because the equivalent shear angle corresponding to 90 mm extension is 30 degrees, which is larger than the maximum shear angle found on the truncated pyramid draping experiments. Therefore, the scatter in the bias-extension tests beyond 90 mm extension was ignored for both the materials, though it should be noted that this is for a specific material in the truncated pyramid shape that this exception was made.

The force-deflection response from simulations matches well with that from experiments as shown in Figure 4. The calibrated shear response from the twill and satin fabrics was then used to validate the fiber shear angle changes observed with the truncated pyramid component.

Following the calibration using the bias-extension experiments and incorporating the bending modulus information previously determined for these fabrics; the input data for the MAT-140 card for the twill fabric was finalized and the parameters are shown in Table I.

The preforming of the fabrics onto the truncated pyramid was then simulated using a single ply of twill fabric and a single ply of satin fabric. The fabric was initially flat and rectangular and cut to proper dimensions to fit the component in its entirety. The fibers in the flat blank were oriented in the global coordinate system with global x-direction as fiber-1 direction. The tools are modeled as rigid bodies with no deformation.

Experimental and Simulated Measurements from the 0/90 Global Orientation

Figure 2d shows a view from above looking at an overall image of the preformed twill fabric in the 0/90 global orientation. It is clearly shown that all four sides draw-in

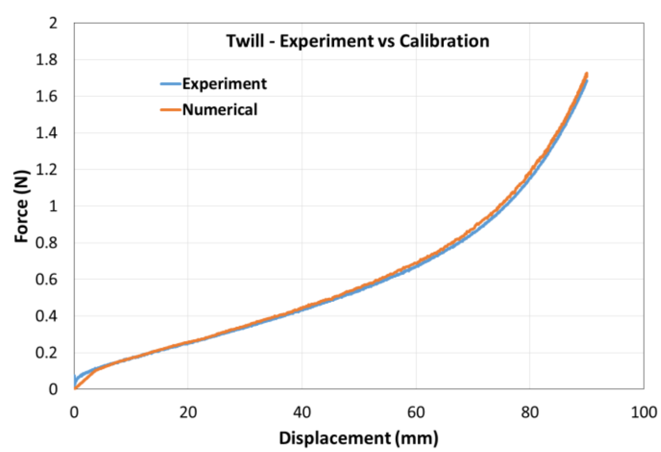

Figure 4. PAM-FORM Output: Force-deflection comparison with experiment

Table I. Material model 140 input data for twill fabric

Fiber Content	0.5
Material Density	1.4 x 10^{-6} Kg/mm^3
Initial Angle Between Fibers	90°
Fiber Direction 1 Tension-Compression Stiffness	Input Stess-Strain Curve
Fiber Direction 1 Bending Stiffness	2 GPa
Fiber Direction 2 Tension-Compression Stiffness	Input Stess-Strain Curve
Fiber Direction 2 Bending Stiffness	2 GPa
In-Plane Shear	Input Stess-Strain Curve

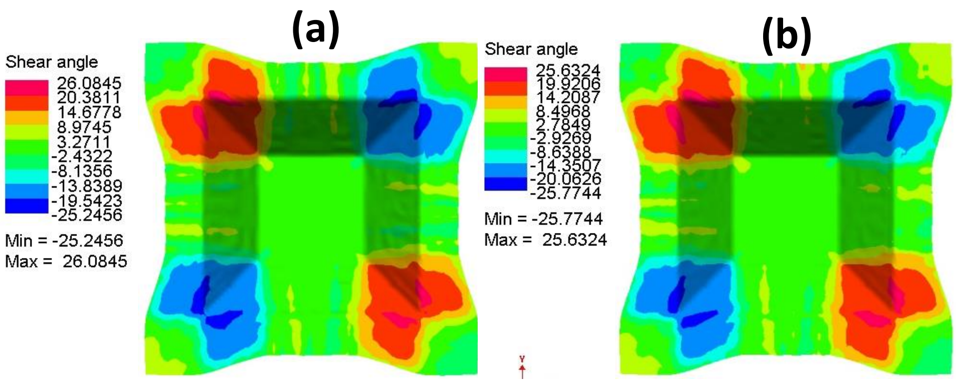

Figure 5. Simulated draw in shapes and fiber shear angle change predictions for fabrics in the 0/90 global orientation. (a) twill fabric and (b) satin fabric.

the same amount. This shape is the same regardless of whether the fabric is twill or satin. The draw in distance is the difference between the original width of the fabric and the deformed line length in the middle of the tool. The corner-to-corner length of the fabric has increased to accommodate the increased line length in this direction. This may be the cause of the fiber shear angle changes in the fabric.

If one examines the shape of the draw-in, it is clear that fibers in the center of the pyramid have adapted to the new shape without changing shear angles. The highest degree of angle change is shown to be the triangular section in the corner of the pyramid where the deformed line length is different for each tow.

Figure 5 shows the simulated ply draw-in shape as well as an overall prediction for the change in fiber shear angle for the different fabrics. Figure 5a is the contour plot for the simulation of the twill fabric in a 0/90° orientation. Figure 5b is the contour plot for the satin fabric in the 0/90° global orientation. From these plots and comparing these shapes to that shown in Figure 2d, it is clear that the simulation was able to capture the overall shape of the fabric following preforming, with the correct draw-in distance and shape. It is also clear that there is not a large difference in the shear angle changes between the different fabrics.

TWILL FABRIC

Figure 6a shows a plot of the absolute value of the shear angle for angles measured on the line closest to the small base of the truncated pyramid with respect to the distance

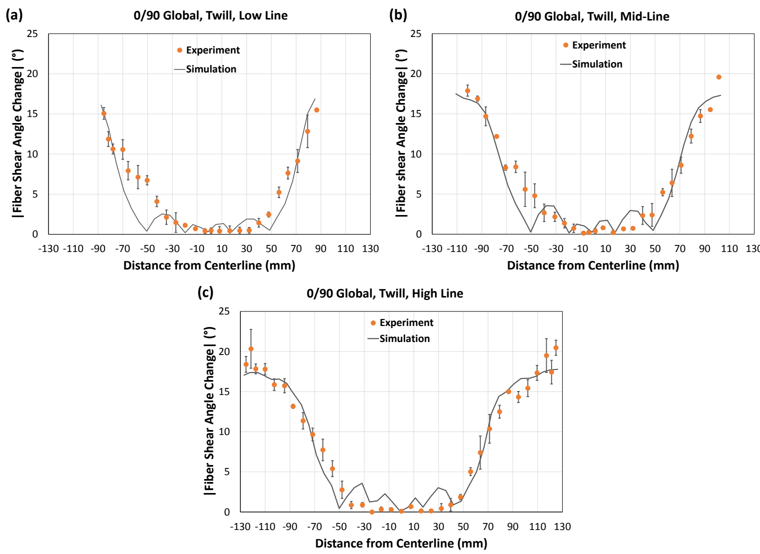

Figure 6. Measured fiber angle changes and predictions for twill fabric deformed in the 0/90 orientation. (a) low line, (b) mid-line, and (c) high line.

from the centerline of the face. Since this line is close to the small base, it does not extend as far to the sides of the centerline as lines closer to the large base of the truncated pyramid. Even though the measurements only extend to roughly 90 mm from the centerline, the measured shear angles go as high as 17° near the edges of the face. The shear angles reduce as we move from the corner toward the centerline, becoming close to zero at the centerline.

This pattern for the measurements continues for the line in the middle of the face (Figure 6b) and the line nearest the large base of the pyramid (Figure 6c). As the measurements continue further from the centerline, the fiber shear angles continue to increase reaching a maximum of 23°. The pattern of the angles is not completely symmetric. This is attributed to the experimental difficulties in perfectly aligning the fabric in its initial global 0/90 orientation.

Figures 6a-c also show the simulated fiber shear angle changes (represented as a line) compared to the experimental measurements (represented as points) for each of the lines on the face of pyramid for the twill fabric. The comparisons between the simulated values and the experimental values are good for this fabric although the simulations tend to fall off somewhat faster than the experimental measurements in the transition between the sides of the face and the center region of the face of the pyramid.

SATIN FABRIC

Figures 7a-c show plots of the measured fiber shear angles for the satin fabric deformed in the 0/90° global orientation. The same trend for the fiber shear angles are noted with this fabric as were observed for the twill fabric. A large region in the center of the pyramid face exhibited unchanged fiber shear angles from the initial angles in the fabric. This then transitions through a region of increasing fiber shear angle leading to the maximum fiber angle change close to the sides of the pyramid face.

Figure 7a shows the plot of the absolute value of the fiber shear angle change for the line closest to the small base of the truncated pyramid. The pattern of the shear angle changes shows a relatively large part of the chart with near zero shear angle change. The shear angles changes start roughly 50 mm on either side of the centerline and continue to increase until the edge of the face is reached. The maximum angle change measured on this line is 14°.

Figure 7b shows the fiber shear angle changes for the horizontal line in the middle of the face of the pyramid. These measurements show the same pattern as that observed for the line near the small base. About 50 mm on either side of the centerline, the fiber shear angle change begins to increase. This increase continues for the full width of the face of the truncated pyramid, increasing to roughly 21°.

The fiber shear angle changes for the line closest to the large base of the pyramid are shown in Figure 7c. This line shows the same pattern as seen with the other two lines on this face of the pyramid. The fiber shear angles begin to change roughly 50 mm on either side of the centerline. The angle changes continue to increase until roughly 110 mm on either side of the centerline. Continuing further toward the edge of the face of the pyramid, the angle changes appear to level off. The maximum fiber angle change for the satin fabric in this starting orientation is 22°, which is essentially the same as the maximum fiber angle change observed with the twill fabric in this orientation.

Figures 7a-c also show the fiber shear angle change predictions in the same manner as previously shown for the twill fabric. As with the twill fabric, the draping predictions for satin fabric were in good agreement with the experiments, actually matching somewhat better in the transition region between the center and the edges of the face for the satin fabric than for the twill fabric.

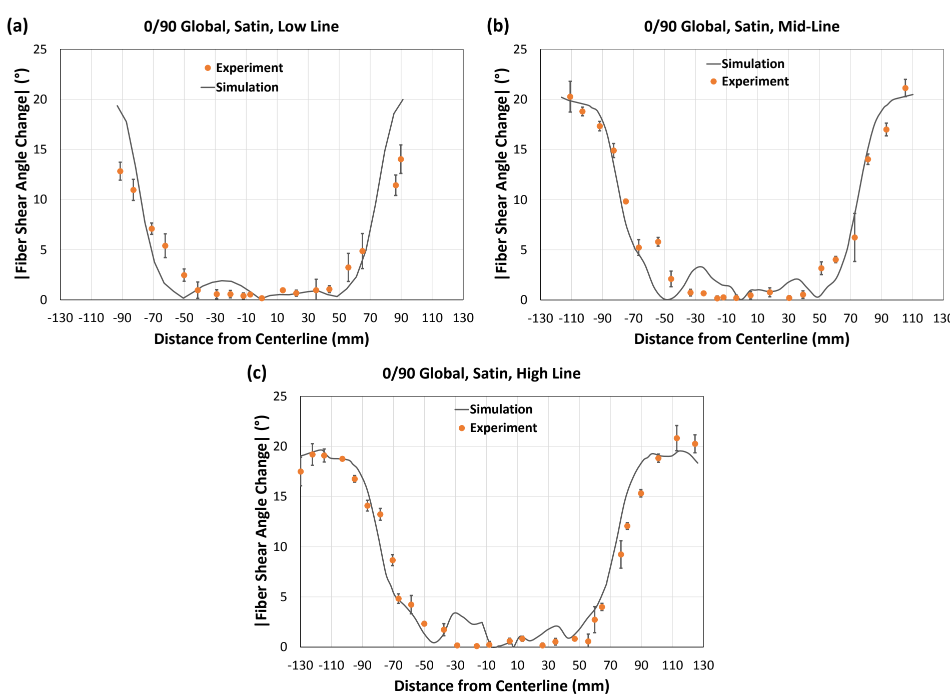

Figure 7. Measured fiber angle changes and predictions for satin fabric in the 0/90 global orientation. (a) low line, (b) mid-line, and (c) high line.

Experimental and Simulated Measurements from a +/- 45° Global Orientation

Figure 8 shows a view from above looking at an overall image of the preformed twill fabric in the +/- 45° global orientation. Unlike the shape exhibited by the 0/90° global orientation, here all four sides draw-in an equal amount. The shape of the fabric after drawing is the same regardless of whether the fabric is twill or satin. The draw-in distance is relatively small. This means that in some manner the increased deformed line length was accommodated by the fabric. Clearly part of this accommodation was through changes to the fiber shear angles. From a practical point of view, it is difficult to precisely place the fabrics at the +/- 45° global orientation during the preforming. Therefore, slight misplacements may also affect the measured fiber shear angles.

Figure 9a and b show the simulated ply draw-in shape as well as an overall prediction for the change in fiber shear angle for twill and the satin fabric respectively when the draping was carried out using fabric in a +/-45° global orientation. When this draw-in shape is compared with that presented in Figure 8, it is clear that the correct draw-in shape has again been predicted for the fabrics starting in this orientation.

TWILL FABRIC

Figure 10a shows the fiber shear angle changes measured following the centerline of the face of the pyramid from the small base to the large base of the pyramid. These measurements shows the trend of generally increasing fiber shear angle differences as the measurements get closer to the large base of the pyramid.

Figures 10b-d show the measurements for the fiber shear angle change on three different lines across the face of the preformed truncated pyramid. Figure 10b shows the values for the line closest to the small base of the pyramid. The measurements from this location are reminiscent of the measurements for the 0/90 global orientation, with the fiber shear angles near the middle of the face changed less than those measurements closer to the edges of the face. The difference between the measurements in these areas is much smaller than that observed with the other orientation.

Figure 8. Top down view of twill fabric deformed from the +/- 45° global orientation.

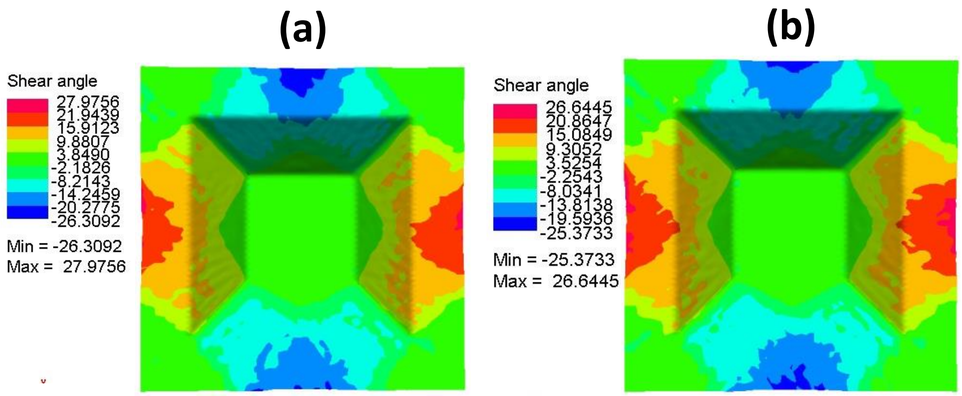

Figure 9. Simulated draw in shapes and fiber shear angle change predictions for fabrics in the +/-45° global orientation. (a) twill fabric and (b) satin fabric.

Figure 10c displays the measurements for a line in the middle of the face of the pyramid. By this point, the difference between the sides and the middle has been mostly eliminated and the angles measured across the face are relatively consistent, averaging about 7°.

Figure 10d shows the measurements for the line closest to the large base of the pyramid. This line contains the largest fiber shear angle changes measured in this orientation, 12°. The angles now have reversed the measurement trend of the line closest to the small base with the angles closer to the edges of the face being somewhat smaller than those measured in the middle of the pyramid face.

In a similar way to the representation for the 0/90 global orientation, Figures 10a-d show the comparison of the simulated fiber shear angle changes to the experimental results for the twill fabric deformed from a +/-45° global orientation. With this orientation, a comparison along the centerline from the small base to the large base of the truncated pyramid is possible. This comparison is shown in Figure 10a. A generally good fit of the simulations to the experimentally measured fiber shear angle changes is observed. There is some discrepancy in the region closer to the small base where the fiber shear angle changes are smaller as it is generally more difficult to measure small angle changes. As the angle changes increase in magnitude, the error bars on the measurements decrease and there is a better match between simulation and experiment.

Figures 10b-d show the comparison of the simulated fiber shear angle changes compared to the experimentally measured fiber shear angle change for the three horizontal lines moving from the small base toward the large base of the pyramid. On comparing the graphs, it is clear that the fiber shear angle changes are smallest near the small base and increase as the measurements progress toward the large base. Figure 10b displays the values for the horizontal line closest to the small base of the pyramid. The general shape and magnitude of the fiber shear angle changes are captured well. The experimental measurements in the middle of the face appear to be somewhat discrepant, but given the error in the experimental measurements for these small angles, this fit is reasonable.

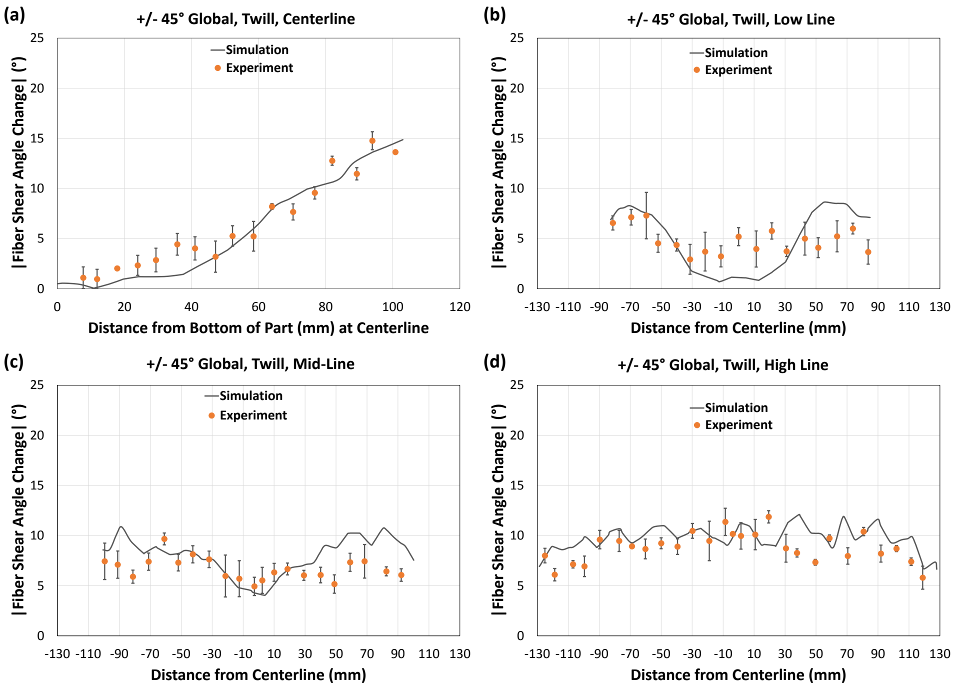

Figure 10. Measured fiber angle changes and predictions for twill fabric deformed in the +/- 45° orientation. (a) Centerline, (b) Low line, (c) Mid-line, and (d) High line.

Figure 10c shows the fiber shear angle change values on a horizontal line midway between the small and the large base of the pyramid. These angle changes are somewhat larger and have smaller error in the measurements. The simulation again captures the correct magnitude of the angle change as well as the pattern of angle change as the measurements move horizontally across the face of the pyramid.

Figure 10d exhibits the fiber shear angle change values measured on a line closer to the large base of the pyramid. It is seen that on this line, the magnitude of the shear angle change again increases and the pattern of the angle changes is somewhat different from the previous lines as the measurements are taken horizontally across the face of the pyramid. In addition, once again the simulation captures these changes well. On all three of the lines, the simulation was able to capture the magnitude of the fiber shear angle change as well as the general shape change of the relative angle changes moving across the face of the pyramid for the twill fabric. The comparison improves as the measurements move closer to the large base, perhaps due to the measured angle changes being larger.

SATIN FABRIC

Figures 11a-d present the measurements collected using when the satin fabric has been preformed over the truncated pyramid tool in a +/-45° orientation. Once again, the same trends were observed with the satin fabric as those that were observed with the twill fabric. The maximum fiber shear angle observed with the satin in this orientation is just over 10°. What is clear is that the trends in the measurements are the same between the fabrics with the low line exhibiting higher angles closer to the edges of the face and the line closest to the large base exhibiting somewhat smaller angles at the

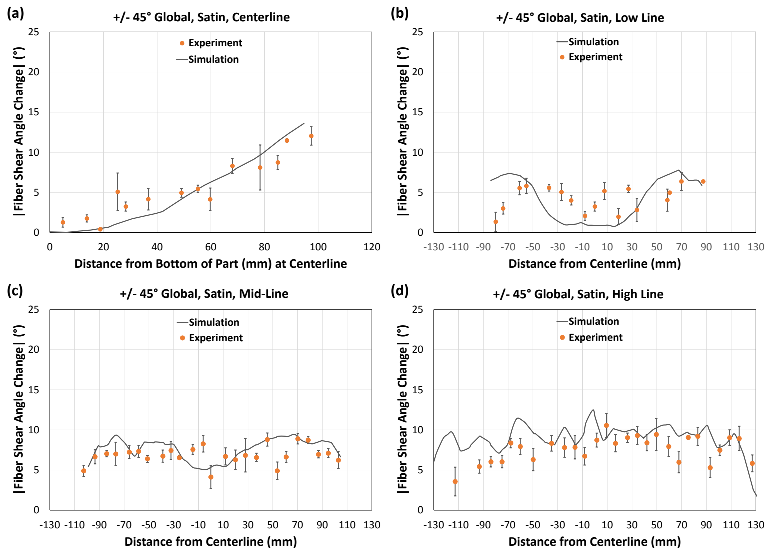

Figure 11. Measured fiber angle changes and predictions for satin fabric deformed in the +/- 45° orientation. (a) Centerline, (b) Low line, (c) Mid-line, and (d) High line.

edges of the face than in the middle. There are no remarkable differences between the measured fiber shear angle changes between the fabrics.

The comparisons of the simulated fiber shear angle changes to the experimentally measured shear angle changes for the satin fabric are also shown in Figures 11a-d. Figure 11a shows the comparison for the measurements along the centerline between the small and large bases of the pyramid. Again, the comparison of the simulated fiber shear angle change to the experimentally measured angle changes is quite good and there appears to be some discrepancy at the low end of the angle change measurements where the experimental measurements are difficult to capture with confidence.

Unfortunately, there are some relatively large errors in some of the measurements. These were due to poor image quality in some areas. However, the comparison between the two sets of results is excellent.

Figure 11b shows the comparison for the horizontal line closest to the small base of the pyramid. These low shear angle changes are particularly difficult to measure, so there is some discrepancy between the two methods particularly in the middle of the face of the pyramid. However, the general shape of the angle change as the measurements move horizontally across the face of the pyramid has been captured by the simulation.

Figure 11c displays the comparison of the experimentally measured fiber shear angle changes to the simulated results for a horizontal line midway between the small base and the large base of the pyramid. As observed with the twill fabric, for the satin fabric the fiber shear angle changes get larger as the measurements are taken closer to the large base. There is again a good match between the two sets of measurements both in magnitude and in shape as the measurement move horizontally across the face of the pyramid.

Figure 11d shows the fiber shear angle changes measured on a horizontal line closer to the large base of the pyramid along with the simulated values for the same line. It appears that the behavior for the measurements along this line are captured by the simulation reasonably well, although there is some over prediction as the measurements get toward the edges of the pyramid face. This appears to be less on one side than the other side. Both measurements also exhibit some evidence of incipient wrinkles due to the fluctuations observed in the shear angle change measurements. These fluctuations are also captured by the simulation.

Sensitivities of the Simulation

The sensitivity of the predicted shear angles with the size of the mesh was also evaluated. Mesh sizes of 2, 3, 5, and 10 mm were evaluated. Essentially no difference was noted between the 2 mm and 3 mm mesh sizes. However, both sizes underpredicted the fiber shear angle changes measured along the centerline for the twill material. A mesh size of 10 mm overpredicted the change in shear angles along the centerline. A 5 mm mesh size was the best for matching the measured change in fiber shear angles.

Since the measured bending stiffness for these materials was significantly higher than expected, ~ 2 GPa, the effect of the bending stiffness on the fiber shear angle change was also investigated by re-running the analysis using a bending modulus of 0.05 GPa. This change in bending modulus made no significant difference in the predicted change in fiber shear angles.

SUMMARY AND NEXT STEPS

The purpose of carrying out this study was to validate the capability of the PAM-FORM computer program for predicting the fiber shear angles observed during the draping of two different fabrics. A truncated pyramid tool was designed and fabricated at the General Motors Research Labs for conducting these experiments. Draping was carried out with the fabric starting in two different global orientations, 0/90° and +/-45°. Predicted shear angles at various location on the draped truncated pyramid were compared with the experimental measurements. While there were some discrepancies with low angle change measurements with both fabrics, overall, this work has shown good agreement between the simulations and the experimentally measured fiber shear angle changes.

For the next phase of validation, the fiber shear angle changes will be predicted using the same calibrated parameters on a larger part, and the effect of these changes will be determined on the physical performance of the part.

ACKNOWLEDGMENTS -

The information, data, or work presented herein was funded in part by the Office of Energy Efficiency and Renewable Energy (EERE), U.S. Department of Energy, under Award Number DE-EE0006826. The information, data, or work presented herein was funded in part by an agency of the United States Government. Neither the United States Government nor any agency thereof, nor any of their employees, makes any warranty, express or implied, or assumes any legal liability or responsibility for the accuracy, completeness, or usefulness of any information, apparatus, product, or process disclosed, or represents that its use would not infringe privately owned rights. Reference herein to any specific commercial product, process, or service by trade name, trademark, manufacturer, or otherwise does not necessarily constitute or imply its endorsement,

recommendation, or favoring by the United States Government or any agency thereof. The views and opinions of authors expressed herein do not necessarily state or reflect those of the United States Government or any agency thereof.

REFERENCES

1. Zhong, T., Hu, H. 2007, "Formability of weft-knitted fabrics on a hemisphere", AUTEX Research Journal, 8(4): 245-251.
2. Chang, S.H., Sharma, S.B., and Sutcliffe, M.P.F. 2003. "Microscopic investigation of tow geometry of a dry satin weave fabric during deformation", Composites Science and Technology, 63: 99-111
3. Lomov, S.V., Barburski, M., Stoilova, Tz., Verpoest, I., Akkerman, R., Loendersloot, R., ten Thije, R.H.W. 2005. "Carbon composites based on multiaxial multiply stitched preforms. Part 3: Biaxial tension, picture frame and compression tests of the preforms", Composites: Part A: Applied Science and Manufacturing, 36(9): 1188–1206.
4. Van Der Weeen, F. 1991. "Algorithms for draping fabrics on doubly-curved surfaces", International Journal for Numerical Methods in Engineering, 31(7): 1415-1426.
5. Vu-Khanh, T., Liu, B. 1995. "Prediction of fiber rearrangement and thermal expansion behavior of deformed woven-fabric laminates", Composites Science and Technology, 53(2): 183-191.
6. Boubaker, B.B., Haussy, B., and Ganghoffer, J.F. 2007. "Discrete models of woven structures. Macroscopic approach," Composites Part B: Engineering, 38(4): 498-505.
7. Yu, W.R., Pourboghrat, F., Chung, K, Zampaloni, M., Kang, T.J. 2002. "Non-orthogonal constitutive equations for woven fabric reinforced thermoplastic composites", Composites, Part A: Applied Science and Manufacturing, 33(8): 1095-1105.
8. Boisse P., Zouari, B., Gasser A. 2005. "A mesoscopic approach for the simulation of woven fibre composite forming", Composites Science and Technology, 65(3-4): pp 429–436.
9. Xue, P., Peng, X., Cao, J. 2003. "A non-orthogonal constitutive model for characterizing woven composites", Composites Part A, Applied Science and Manufacturing, 34(2): 183-193.
10. Mathieu, S., Hamila, N., Bouillon, F., Boisse, P. 2015. "Enhanced modeling of 3D composite preform deformation taking into account local fiber bending stiffness", Composites Science and Technology, 117: 323-333.
11. Badel, P., Vidal-Salle, E., Boisse. 2008. "Large deformation analysis of fibrous materials using rate constitutive equations", Computers and Structures, 86: 1164-1175.
12. Wang, Y., Sun, X. 2001. "Digital-element simulation of textile processes", Composites Science and Technology, 61: 311-319.
13. Daelemans, L., Faes, J., Allaoui, S., Hivet, G., Dierick, M., Van Hoorebeke, L., Van Paepegem, W. 2016. "Finite element simulation of woven geometry and mechanical behavior of a 3D woven dry fabric under tensile and shear loading using digital element method", Composites Science and Technology, 137: 177-187.
14. Harrison, P., Clifford, M.J., Long, A.C. 2004. "Shear characterization of viscous woven textile composites: a comparison between picture frame and bias extension experiments", Composites Science and Technology, 64: 1453-1465.
15. Schneider, C.A., Rasband, W.S., Eliceiri, K.W. 2012. "NIH Image to ImageJ: 25 years of image analysis," Nature Methods 9: 671-675.
16. Rodgers, W.R., Jin, X., Zhu, J., Wathen, T., Doroudian, M., Aitharaju, V. 2016. "Draping Simulation of Woven Fabrics", Presented at the SPE Automotive Composites Conference & Exposition, Novi, Michigan, September 7-9, 2016